

Melting behavior of large disordered sodium clusters.

Andrés Aguado

Departamento de Física Teórica, Universidad de Valladolid, Valladolid 47011, Spain

The melting-like transition in disordered sodium clusters Na_N , with $N=92$ and 142 is studied by using a first-principles constant-energy molecular dynamics simulation method. Na_{142} , whose atoms are distributed in two (surface and inner) main shells with different radial distances to the center of mass of the cluster, melts in two steps: the first one, at ≈ 130 K, is characterized by a high intrashell mobility of the atoms, and the second, homogeneous melting, at ≈ 270 K, involves diffusive motion of all the atoms across the whole cluster volume (both intrashell and intershell displacements are allowed). On the contrary, the melting of Na_{92} proceeds gradually over a very wide temperature interval, without any abrupt step visible in the thermal or structural melting indicators. The occurrence of well defined steps in the melting transition is then shown to be related to the existence of a distribution of the atoms in shells. Thereby we propose a necessary condition for a cluster to be considered rigorously amorphouslike (totally disordered), namely that there are no space regions of the cluster where the local value of the atomic density is considerably reduced. Na_{92} is the only cluster from the two considered that verifies this condition, so its thermal behavior can be considered as representative of that expected for amorphous clusters. Na_{142} , on the other hand, has a discernible atomic shell structure and should be considered instead as just partially disordered. The thermal behavior of these two clusters is also compared to that of icosahedral (totally ordered) sodium clusters of the same sizes.

PACS numbers: 36.40.Ei 64.70.Dv

I. INTRODUCTION

Cluster melting is a topic of current theoretical^{1–7} and experimental^{8–11} interest, motivated by the observation of several size-dependent properties which have no analog in the bulk phase. Between those properties, we can mention the following: (i) the melting like transition does not occur at a well defined temperature as in the solid, but spreads over a finite temperature interval that widens as the cluster size decreases. The lower end of that interval defines the freezing temperature T_f below which the cluster is completely solidlike, their constituent atoms just vibrating about their equilibrium positions. The upper part of the interval defines the melting temperature above which all the atoms can diffuse across the cluster and the “liquid” phase is completely established. Between those two temperatures the cluster is not fully solid nor fully liquid.¹² It is in that transition region where the cluster-specific behavior emerges: (ia) Premelting effects like partial melting of the cluster (the most usual case is surface melting)¹³ or structural isomerizations upon heating, which lead to a melting in steps.¹⁴ (ib) The dynamic coexistence regime, where the cluster can fluctuate in time between being completely solid or liquid.¹⁵ (ii) Strong nonmonotonic variations of the melting temperature with size have been found in recent experiments on sodium clusters.⁹ The maxima in the melting temperature are not in exact correspondence with either electronic or atomic shell closing numbers, but bracketed by the two, suggesting that both effects are relevant to the melting process. It is important to note that the values of T_f and T_m as defined above are not yet amenable

to the experiments, and that the experimental melting temperature is somewhere between these two values.

Previously^{6,7} we have reported density functional orbital-free molecular dynamics (OFMD) simulations of the melting process in sodium clusters Na_N , with $N=8, 20, 55, 92$, and 142 . The OFMD technique¹⁶ is completely analogous to the method devised by Car and Parrinello (CP) to perform dynamic simulations at an *ab initio* level,¹⁷ but the electron density is taken as the dynamic variable,¹⁸ as opposed to the Kohn-Sham (KS) orbitals¹⁹ in the original CP method. This technique has been already used both in solid state^{20,21} and cluster^{2,22,23} physics. In contrast to simulations which use empirical interatomic potentials, the detailed electronic structure and the electronic contribution to the energy and the forces on the ions are recalculated efficiently every atomic time-step. The main advantage over KS-based methods is that the computational effort to update the electronic system increases linearly with the cluster size N , in contrast to the N^3 scaling of orbital-based methods. Indeed, these were the first molecular dynamics simulations of large clusters as Na_{92} and Na_{142} that included an explicit treatment of the electronic degrees of freedom.

A very important issue in the simulations of cluster melting is the election of the low-temperature isomer to be heated. A good knowledge of the ground state structure (global minimum) is required, as the details of the melting transition are known to be isomer-dependent.²⁴ But the problem of performing a realistic global optimization search is exponentially difficult as size increases, so finding the global minima of Na_{92} and Na_{142} becomes im-

practical. In our previous work⁷ we directly started from icosahedral isomers, as there is some experimental⁸ and theoretical²⁵ indications that suggest icosahedral packing in sodium clusters, and found a good agreement with the experimental results of Haberland's group.⁹ However, we were unable to find those icosahedral structures by an unconstrained search method as simulated annealing, which always led to disordered isomers both for Na₉₂ and Na₁₄₂. Although the icosahedral structures are more stable in all the cases, the energy difference between both isomers is approximately 0.02 eV/atom, which is very small. Amorphouslike structures have been found recently to be the ground state isomers of gold clusters for a number of sizes,^{26,27} and pair potential calculations performed by Doye and Wales predict that the amorphous state is favored by long potential ranges.²⁸ The specific features of those structures are little or no spatial symmetry and a pair distribution function typical of glasses. Besides that, one usually finds a large number of amorphouslike isomers nearly degenerate in energy, which suggests that they occupy a substantial fraction of the phase space available to the cluster. Both the energy proximity to the more stable icosahedral isomers and the large entropy associated with the amorphous part of the phase space make plausible that amorphous isomers could be present in the experimental cluster beams, so their thermal properties deserve specific investigation. Apart from this, the study of melting in amorphouslike clusters is intrinsically interesting from a theoretical point of view. Thus, the goals of this work are to study the mechanisms by which the melting-like transition proceeds in two disordered isomers of Na₉₂ and Na₁₄₂, to study the influence on the melting behavior of the disorder degree, and to make a meaningful comparison with the melting behavior of the corresponding icosahedral isomers. In the next section we briefly present some technical details of the method. The results are presented and discussed in section III and, finally, section IV summarizes our main conclusions.

II. THEORY

The orbital-free molecular dynamics method is a Car-Parrinello total energy scheme¹⁷ which uses an explicit kinetic-energy functional of the electron density, and has the electron density as the dynamical variable, as opposed to the KS single particle wavefunctions. The main features of the energy functional and the calculation scheme have been described at length in previous work,^{16,22,2,6} and details of our method are as described by Aguado et al.⁶ In brief, the electronic kinetic energy functional of the electron density, $n(\vec{r})$, corresponds to the gradient expansion around the homogeneous limit through second order^{18,29–31}

$$T_s[n] = T^{TF}[n] + \frac{1}{9}T^W[n], \quad (1)$$

where the first term is the Thomas-Fermi functional (Hartree atomic units have been used)

$$T^{TF}[n] = \frac{3}{10}(3\pi^2)^{2/3} \int n(\vec{r})^{5/3} d\vec{r}, \quad (2)$$

and the second is the lowest order gradient correction, where T^W , the von Weizsäcker term, is given by

$$T^W[n] = \frac{1}{8} \int \frac{|\nabla n(\vec{r})|^2}{n(\vec{r})} d\vec{r}. \quad (3)$$

The local density approximation is used for exchange and correlation.^{32,33} In the external field acting on the electrons, $V_{ext}(\vec{r}) = \sum_n v(\vec{r} - \vec{R}_n)$, we take v to be the local pseudopotential of Fiolhais *et al.*,³⁴ which reproduces well the properties of bulk sodium and has been shown to have good transferability to sodium clusters.³⁵ The cluster is placed in a unit cell of a cubic superlattice, and the set of plane waves periodic in the superlattice is used as a basis set to expand the valence density. Following Car and Parrinello,¹⁷ the coefficients of that expansion are regarded as generalized coordinates of a set of fictitious classical particles, and the corresponding Lagrange equations of motion for the ions and the electron density distribution are solved as described in Ref. 6.

The calculations used a supercell of edge 71 a.u. and the energy cut-off in the plane wave expansion of the density was 8 Ryd. In all cases, a 64×64×64 grid was used. Previous tests^{6,7} indicate that the cut-offs used give good convergence of bond lengths and binding energies. The fictitious mass associated with the electron density coefficients ranged between 1.0×10^8 and 3.3×10^8 a.u., and the equations of motion were integrated using the Verlet algorithm³⁶ for both electrons and ions with a time step ranging from $\Delta t = 0.73 \times 10^{-15}$ sec. for the simulations performed at the lowest temperatures, to $\Delta t = 0.34 \times 10^{-15}$ sec. for those at the highest ones. These choices resulted in a conservation of the total energy better than 0.1 %.

Several molecular dynamics simulation runs at different constant energies were performed in order to obtain the caloric curve for each cluster. The initial positions of the atoms for the first run were taken by slightly deforming the equilibrium low temperature geometry of the cluster. The final configuration of each run served as the starting geometry for the next run at a different energy. The initial velocities for every new run were obtained by scaling the final velocities of the preceding run. The total simulation times varied between 8 and 18 ps for each run at constant energy.

A number of indicators to locate the melting-like transition were employed. Namely, the specific heat defined by³⁷

$$C_v = [N - N(1 - \frac{2}{3N-6}) < E_{kin} >_t < E_{kin}^{-1} >_t]^{-1}, \quad (4)$$

where N is the number of atoms and $\langle \rangle_t$ indicates the average along a trajectory; the time evolution of the distance between each atom and the center of mass of the cluster

$$r_i(t) = |\vec{R}_i(t) - \vec{R}_{cm}(t)|; \quad (5)$$

the average over a whole dynamical trajectory of the radial atomic distribution function $g(r)$, defined by

$$dN_{at} = g(r)dr \quad (6)$$

where $dN_{at}(r)$ is the number of atoms at distances from the center of mass between r and $r + dr$; and finally, the diffusion coefficient

$$D = \frac{1}{6} \frac{d}{dt} (\langle r^2(t) \rangle), \quad (7)$$

which is obtained from the long time behavior of the mean square displacement $\langle r^2(t) \rangle = \frac{1}{Nn_t} \sum_{j=1}^{n_t} \sum_{i=1}^N [\vec{R}_i(t_{0j} + t) - \vec{R}_i(t_{0j})]^2$, where n_t is the number of time origins, t_{0j} , considered along a trajectory.

III. RESULTS

The most stable disordered structures of Na_{92} and Na_{142} that we have found with the simulated annealing technique are shown in Fig. 1, together with the relaxed icosahedral isomers obtained as explained in our previous work.⁷ The dynamical annealing runs¹⁷ were started from high-temperature liquid isomers thermalized during 30 ps at 600 K. The cooling strategy was to reduce the internal cluster temperature by a factor of 0.9999 of its actual value each twelve atomic time steps. With the chosen time step of 0.34×10^{-15} sec. the temperature reduction is applied each four femtoseconds. A first important difference between the icosahedral and disordered isomers is that the former ones have a smoother surface. Besides that, no apparent spatial symmetry is observed in the disordered isomers. In Fig. 2 we show the short-time averages (sta) of the distances between each atom and the center of mass of the cluster for both isomers of Na_{142} , obtained from an OFMD run at a low temperature. The values of $\langle r_i(t) \rangle_{sta}$ are almost independent of time. The clusters are solid, the atoms merely vibrating around their equilibrium positions. Curve crossings are due to oscillatory motion and slight structural relaxations rather than diffusive motion. The difference between Figs. 2a and 2b is due to structure. For the icosahedral isomer in Fig. 2a one can distinguish quasidegenerate groups which are characteristic of the symmetry: one line near the center of mass of the cluster identifies the central atom, whose position does not exactly coincide with the center of mass because of the location of the five surface vacancies (147 atoms are needed to form a complete three-shell icosahedron); 12 lines correspond to the first icosahedral shell; another 42 complete the second shell,

within which we can distinguish the 12 vertex atoms from the rest because their distances to the center of mass are slightly larger; finally, 82 lines describe the external shell, where again we can distinguish the 7 vertex atoms from the rest. In contrast, the lines for the disordered isomer in Fig. 2b are quite dispersed. Nevertheless, there is a narrow interval where the ionic density is very low, that serves to define separate surface and inner atomic shells. The case of Na_{92} (not shown) is similar, but in that case the structure is more uniformly amorphous, and there is no way to distinguish between surface and inner shells. We will see below that this small difference is very important. Soler *et al.*^{26,27} have compared the structures of icosahedral and amorphous gold clusters, with similar results: while the atoms in the icosahedral isomers are clearly distributed in atomic shells with different radial distances to the center of mass of the cluster, in the case of amorphous clusters there are “atomic transfers” between shells that blur the atomic shell structure. In the case of gold clusters, the amorphous isomers turn out to be the minimum energy structures for a number of sizes.²⁶ In the case of Na_{92} and Na_{142} , the icosahedral isomers are more stable than the lowest energy disordered isomers found (0.017 eV/atom and 0.020 eV/atom for Na_{92} and Na_{142} respectively).⁷

For each cluster we have calculated the internal temperature, defined as the average of the ionic kinetic energy,³⁷ as a function of the total energy—the so-called caloric curve. A thermal phase transition is indicated in the caloric curve by a change of slope, the slope being the specific heat; the height of the step gives an estimate of the latent heat of fusion. However, melting processes are more easily recognized as peaks in the specific heat as a function of temperature, that has been calculated directly from eq. (4). The fact that the specific heat peaks occur at the same temperatures as the slope changes of the caloric curve (see curves below) gives us confidence on the convergence of our results, as those two quantities have been obtained in different ways.

The specific heat curves for Na_{142} (fig. 3) display two main peaks, suggestive of a two-step melting process. For the disordered cluster the two peaks are well separated in temperature, $T_s^{dis} \approx 130$ K and $T_m^{dis} \approx 270$ K, whereas they are much closer together for the icosahedral cluster, $T_s^{ico} \approx 240$ K and $T_m^{ico} \approx 270$ K, so close that only one slope change in the caloric curve can be distinguished in this case. The results suggest that the melting transition starts at a temperature T_s and finishes at T_m with the difference in the melting of the two isomers being the smaller T_s value of the disordered isomer. In our previous work⁷ we showed that for the icosahedral cluster those two steps are due to surface melting and homogeneous melting, respectively. Here we show that a similar explanation is valid for the disordered Na_{142} isomer. At $T=160$ K, a temperature between T_s^{dis} and T_m^{dis} , the structure of the disordered cluster is more fluid than at low temperature (fig. 2). Fig. 4 indicates that the spherical atomic shells have separately melted, atoms undergoing diffu-

sive motions mainly across a given shell, as seen in the bold lines, without an appreciable intershell diffusion (although some occasional intershell displacement has been observed). The larger spread of the upper bold line indicates that diffusion is appreciably faster in the surface shell. Thus the transition at 130 K can be identified with intrashell melting. Why it occurs at a rather low temperature is associated with the large spread in the radial distances of the atoms in each shell. The atomic shells are structurally disordered at low temperature, although kinetically frozen, like in a typical glass, so inducing diffusion in the shells of that cluster is rather easy and occurs at moderate temperatures. The surface melting stage does not develop in the icosahedral isomer until a temperature of $T_s^{ico} \approx 240$ K is reached. At this temperature, the time evolution of the surface atomic distances to the cluster center becomes very similar to those of the disordered Na_{142} isomer at 160 K.⁷ Inducing diffusion in the surface of the icosahedral isomer requires a higher temperature because of the higher structural order of its surface. Once the surface of both isomers has melted, homogeneous melting occur at the same temperature, ≈ 270 K, in very good agreement with the experimental value of 280 K.⁹ From that temperature on, the liquid phase is completely established (all atoms can diffuse across the whole cluster volume)⁷ and differences between both isomers have no sense anymore.

The thermal behavior of both isomers is not so different. The radial atomic density distribution of the disordered isomer at 160 K (Fig. 5) shows a smoothed shape with respect to that found at low T, but a distribution of the atoms in separate surface and inner atomic shells can be clearly distinguished. In fact, the intermediate temperature distribution is similar to that found for the icosahedral isomer in the same temperature region,⁷ as the atomic shells are equally distinguished. The small gap in the ionic density (Figs. 2 and 5) of the disordered isomer at low temperature drives the cluster towards a well defined shell structure upon heating. We conclude that, despite the high orientational disorder in both surface and inner shells, the cluster can not be considered completely amorphous, as Fig. 5 at intermediate temperature shows some radial atomic ordering. There are still more similarities. The solidlike phase of the icosahedral isomer disappears as soon as a temperature of 130 K is reached, even though no peak in the specific heat is detected: there are isomerization transitions between different permutational isomers which preserve the icosahedral structure.⁷ These isomerizations involve the displacement of the five surface vacancies across the outer shell. Thus, both isomers leave the solidlike phase at ≈ 130 K, the only difference being that one has direct access to the intrashell melting stage while the other enters first an isomerization regime. Calvo and Spiegelmann⁵ have related the appearance of specific heat peaks to sudden openings of the available phase space. In the isomerization regime the icosahedral cluster has access just to a limited number of symmetry-equivalent isomers, while

the phase structure of the disordered cluster opens suddenly to include a very large number of isomers, as all the possible position interchanges between two atoms of a given shell are allowed. Thus, a specific heat peak appears at $T \approx 130$ K for the disordered isomer, but not for the icosahedral isomer. Any atomic shell distribution in the time average of $g(r)$ disappears completely when homogeneous melting occur (Fig. 5).

The results for Na_{92} are shown in fig. 6. Two-step melting is again observed in the icosahedral isomer, with a small prepeak in the specific heat at $T_s^{ico} \approx 130$ K and a large peak, corresponding to homogeneous melting, at $T_m^{ico} \approx 240$ K. In this case T_s^{ico} and T_m^{ico} are well separated. T_s^{ico} is in the range where the isomerization processes in icosahedral Na_{142} set in and the intrashell melting stage in disordered Na_{142} develops. The larger number of vacancies in the surface shell of icosahedral Na_{92} , as compared to icosahedral Na_{142} , allows for true surface diffusion and these processes give rise to a distinct peak in the specific heat.⁷ The disordered isomer melts gradually over a wide temperature interval, and no prominent specific heat peaks nor important slope changes in the caloric curve are detected. Ercolessi *et al.*³⁸ have also found a melting process without a latent heat of fusion for amorphous gold clusters with less than ~ 90 atoms. In Fig. 7 we show the radial ionic density distribution of disordered Na_{92} at several representative temperatures. At a temperature as low as 70 K there is no discernible atomic shell structure. The $g(r)$ function for a higher temperature where the surface of the icosahedral isomer has already melted is not very different. At a temperature where the icosahedral isomer is liquid the only appreciable change in $g(r)$ is due to the thermal expansion of the cluster. The structure of cold disordered Na_{92} is both radially and orientationally disordered. The structure is kinetically frozen, but there seems to be no barriers impeding the exploration of the liquid part of the phase space. In fact, the cluster is already in that region at low temperature, as Fig. 7 shows. This is seen most clearly in the evolution of the diffusion behavior with temperature. In Fig. 8 we show the temperature variation of the square root of the diffusion coefficient. While the two steps in the melting of the icosahedral isomer are clearly detected as slope changes at the corresponding temperatures, the value of \sqrt{D} for the disordered isomer increases with temperature in a smooth way, without any abrupt change. Thus, the opening of the available phase space proceeds in a gradual way and specific heat peaks are not detected.

We have found a very different thermal behavior for two clusters that were classified in principle as disordered. Although just two examples are not enough to draw general conclusions, we believe that the thermal behavior typical of amorphouslike sodium clusters is that found for Na_{92} , and that what is lacking is a clear definition of what an amorphous cluster is. In line with the discussion of “atomic transfers” between shells advanced by Soler *et al.*²⁷ we propose that a large orientational

disorder is not enough for a cluster to be classified as amorphouslike. Only when those atomic transfers are maximal, in such a way that no local regions with low atomic density exist, the cluster can be considered completely amorphous. The existence of those regions, however small they may be (as is the case of Na₁₄₂), promote the creation of appreciable free energy barriers in the potential energy surface, so sudden access to a substantial region of the available phase space is expected above a certain temperature, and peaks will appear in the temperature evolution of the specific heat. On the contrary, the absence of such low atomic density regions facilitates the diffusion of the atoms across the whole cluster volume right from the start of the heating process. As the liquidlike phase is established precisely when all the atoms in the cluster can diffuse across the cluster volume, we expect that no appreciable free energy barriers will be found in these cases, and no specific heat peaks will be detected.

A few comments regarding the quality of the simulations and of the annealing runs are perhaps in order here. The orbital-free representation of the atomic interactions is much more efficient than the more accurate KS treatments, but is still substantially more expensive computationally than a simulation using phenomenological many-body potentials. Such potentials contain a number of parameters that are usually chosen by fitting some bulk and/or molecular properties. In contrast our model is free of external parameters, although there are approximations in the kinetic and exchange-correlation functionals. The orbital-free scheme accounts, albeit approximately, for the effects of the detailed electronic distribution on the total energy and the forces on the ions. We feel that this is particularly important in metallic clusters for which a large proportion of atoms are on the surface and experience a very different electronic environment than an atom in the interior. Furthermore, the adjustment of the electronic structure and consequently the energy and forces to rearrangements of the ions is also taken into account. But the price to be paid for the more accurate description of the interactions is a less complete statistical sampling of the phase space. The simulation times are substantially shorter than those that can be achieved in phenomenological simulations. The cooling rate employed in the annealing runs is also faster than those that can be achieved by using empirical potentials. Nevertheless, we expect that the locations of the several transitions are reliable, because all the indicators we have used, both thermal and structural ones, are in essential agreement on the temperature at which the transitions start. On the other hand, the disordered isomers found in different annealing runs did not show substantial structural or energetic differences with respect to those studied here.

IV. SUMMARY

The melting-like transition in disordered Na₁₄₂ and Na₉₂ has been investigated by applying an orbital-free, density-functional molecular dynamics method. The computational effort which is required is modest in comparison with the traditional Car-Parrinello Molecular Dynamics technique based on Kohn-Sham orbitals, that would be very costly for clusters of this size. This saving allows the study of large clusters.

A disordered isomer of Na₁₄₂ melts in two steps as evidenced by the thermal indicators. The transition at $T_s^{dis} \approx 130$ K is best described as intrashell melting. This is followed at $T_m^{dis} \approx 270$ K by homogeneous melting. Melting is found to depend on the starting low-temperature isomer. Specifically, for an icosahedral Na₁₄₂ isomer, the analysis of thermal, macroscopic properties places those two stages much closer in temperature, 240 K and 270 K respectively.⁷ Nevertheless, isomerization transitions are observed in the icosahedral isomer at a temperature as low as $T_s^{dis} \approx 130$ K. These isomerizations involve the motion of the five atomic vacancies in the cluster surface, preserve the icosahedral structure and do not give rise to any pronounced feature in the caloric curve. In the disordered isomer there is not a separate isomerization regime (something rather evident because there is not an underlying ordered structure in each shell), but there is a melting-in-steps process, due to the distribution of the atoms in different shells. Thus, the melting of both isomers is not as different as suggested by the thermal indicators. An icosahedral isomer of Na₉₂ melts also in a similar way: there is a minor peak in C_v at $T_s^{ico} \approx 130$ K that indicates surface melting, and a main, homogeneous melting peak at $T_m^{ico} \approx 240$ K. The lower value of T_s^{ico} , as compared to Na₁₄₂, is due to the larger number of surface vacancies, and the melting-in-step process is due to the atomic shell structure. The melting of disordered Na₉₂ proceeds instead gradually, and spreads over a very wide temperature interval. The thermal indicators as the caloric curve or the specific heat do not show any indications of an abrupt transition, which suggests that the phase space available to the cluster does not increases suddenly at any given temperature. The square root of the diffusion coefficient increases with temperature in a smooth way, in contrast to the step diffusive behavior of icosahedral Na₉₂. It has been suggested that the absence of any abrupt transition is closely related to the absence of any shell structure in the radial atomic density distribution, which should be considered a necessary condition for a cluster to be considered completely amorphous. In this, sense, only the disordered isomer of Na₉₂ can be considered rigorously amorphous, while the disordered Na₁₄₂ isomer should be considered just partially amorphous.

In summary, we have found a number of structural properties that have an important effect on the melting properties of sodium clusters. A melting in steps pro-

cess is to be expected in almost all clusters where a clear distribution of the atoms in radial shells exists, as is the case of both isomers of Na₁₄₂ and of the icosahedral isomer of Na₉₂. In those cases, intrashell diffusive motion starts at a temperature T_{*intra*}, lower than the temperature T_{*inter*} at which intershell diffusive motion begins to be important. The difference T_{*inter*}-T_{*intra*} is small if the orientational order of the shells is large (for example, icosahedral order) and the number of vacancies in each shell is small: this occurs for icosahedral Na₁₄₂, with just five surface vacancies; A limit case is icosahedral Na₅₅. With two complete atomic shells, intrashell motions are as difficult as intershell motions and the two transitions merge into one.⁷ When one shell contains a large number of vacancies, the two temperatures are well separated no matter how high the orientational order is: this is exemplified by the case of icosahedral Na₉₂. Also, if the shells have a high orientational disorder, the two transitions are well separated in temperature no matter how close we are from an icosahedral shell closing: an example is the disordered Na₁₄₂ isomer. Finally, a gradual melting process without any abrupt transition is to be expected for all those clusters which have both orientational and radial disorder, that is for amorphouslike clusters: this is the case of amorphous Na₉₂.

ACKNOWLEDGMENTS: This work has been supported by DGES (Grant PB98-0368) and Junta de Castilla y León (VA70/99). The author acknowledges useful discussions with J. M. López, J. A. Alonso, and M. J. Stott.

Captions of Figures.

Figure 1 Structures of the low temperature (a) amorphous Na₁₄₂, (b) icosahedral Na₁₄₂, (c) amorphous Na₉₂ and (d) icosahedral Na₉₂ isomers.

Figure 2 Short-time averaged distances $\langle r_i(t) \rangle_{sta}$ between each atom and the center of mass in Na₁₄₂, as functions of time for (a) the icosahedral isomer at T= 30 K and (b) the amorphous isomer at T= 47 K.

Figure 3 Caloric and specific heat curves of Na₁₄₂, taking the internal cluster temperature as the independent variable. The deviation around the mean temperature is smaller than the size of the circles.

Figure 4 Short-time averaged distances $\langle r_i(t) \rangle_{sta}$ between each atom and the center of mass in amorphous Na₁₄₂ as functions of time at T= 160 K. The bold lines follow the evolution of a particular atom in the surface shell and another in the outermost core shell.

Figure 5 Time averaged radial atomic density distribution of the amorphous isomer of Na₁₄₂, at some representative temperatures.

Figure 6 Caloric and specific heat curves of Na₉₂, taking the internal cluster temperature as the independent variable. The deviation around the mean temperature is smaller than the size of the circles.

Figure 7 Time averaged radial atomic density distribution of the amorphous isomer of Na₉₂, at some representative temperatures.

Figure 8 Square root of the diffusion coefficient as a function of temperature for the icosahedral and amorphous isomers of Na₉₂.

- ¹ A. Bulgac and D. Kusnezov, Phys. Rev. Lett. **68**, 1335 (1992); Phys. Rev. B **45**, 1988 (1992); N. Ju and A. Bulgac, Phys. Rev. B **48**, 2721 (1993); M. Fosmire and A. Bulgac, *ibid.* **52**, 17509 (1995); J. M. Thompson and A. Bulgac, *ibid.* **40**, 462 (1997); L. J. Lewis, P. Jensen, and J. L. Barrat, *ibid.* **56**, 2248 (1997); S. K. Nayak, S. N. Khanna, B. K. Rao, and P. Jena, J. Phys.: Condens. Matter **10**, 10853 (1998). F. Calvo and P. Labastie, J. Phys. Chem. B **102**, 2051 (1998); J. P. K. Doye and D. J. Wales, Phys. Rev. B **59**, 2292 (1999); J. Chem. Phys. **111**, 11070 (1999).
- ² P. Blaise, S. A. Blundell, and C. Guet, Phys. Rev. B **55**, 15856 (1997).
- ³ A. Rytkönen, H. Häkkinen, and M. Manninen, Phys. Rev. Lett. **80**, 3940 (1998).
- ⁴ C. L. Cleveland, W. D. Luedtke, and U. Landman, Phys. Rev. Lett. **81**, 2036 (1998); Phys. Rev. B **60**, 5065 (1999).
- ⁵ F. Calvo and F. Spiegelmann, Phys. Rev. Lett. **82**, 2270 (1999); J. Chem. Phys. **112**, 2888 (2000).
- ⁶ A. Aguado, J. M. López, J. A. Alonso, and M. J. Stott, J. Chem. Phys. **111**, 6026 (1999);
- ⁷ J. Phys. Chem. B, submitted (preprint available at <http://xxx.lanl.gov/abs/physics/9911042>).
- ⁸ T. P. Martin, Phys. Rep. **273**, 199 (1996).
- ⁹ M. Schmidt, R. Kusche, W. Kronmüller, B. von Issendorff, and H. Haberland, Phys. Rev. Lett. **79**, 99 (1997); M. Schmidt, R. Kusche, B. von Issendorff, and H. Haberland, Nature **393**, 238 (1998); R. Kusche, Th. Hippler, M. Schmidt, B. von Issendorff, and H. Haberland, Eur. Phys. J. D **9**, 1 (1999).
- ¹⁰ M. Schmidt, C. Ellert, W. Kronmüller, and H. Haberland, Phys. Rev. B **59**, 10970 (1999).
- ¹¹ H. Haberland, in "Metal Clusters", ed. W. Ekardt (John Wiley & Sons, 1999), p. 181.
- ¹² J. Jellinek, T. L. Beck, and R. S. Berry, J. Chem. Phys. **84**, 2783 (1986).
- ¹³ Z. B. Güvenc and J. Jellinek, Z. Phys. D **26**, 304 (1993).
- ¹⁴ V. K. W. Cheng, J. P. Rose, and R. S. Berry, Surf. Rev. Lett. **3**, 347 (1996).
- ¹⁵ H. P. Cheng and R. S. Berry, Phys. Rev. A **45**, 7969 (1991); R. S. Berry, in *Clusters of Atoms and Molecules*, edited by H. Haberland (Springer, Berlin, 1994), pp. 187–204.
- ¹⁶ M. Pearson, E. Smargiassi, and P. A. Madden, J. Phys.: Condens. Matter **5**, 3221 (1993).
- ¹⁷ R. Car and M. Parrinello, Phys. Rev. Lett. **55**, 2471 (1985); M. C. Payne, M. P. Teter, D. C. Allan, T. A. Arias, and J. D. Joannopoulos, Rev. Mod. Phys. **64**, 1045 (1992).
- ¹⁸ P. Hohenberg and W. Kohn, Phys. Rev. **136**, 864B (1964).
- ¹⁹ W. Kohn and L. J. Sham, Phys. Rev. **140**, 1133A (1965).

²⁰ E. Smargiassi and P. A. Madden, Phys. Rev. B **49**, 5220 (1994); M. Foley, E. Smargiassi, and P. A. Madden, J. Phys.: Condens. Matter **6**, 5231 (1994); E. Smargiassi and P. A. Madden, Phys. Rev. B **51**, 117 (1995); *ibid.* **51**, 129 (1995); M. Foley and P. A. Madden, *ibid.* **53**, 10589 (1996); B. J. Jesson, M. Foley, and P. A. Madden, *ibid.* **55**, 4941 (1997); J. A. Anta, B. J. Jesson, and P. A. Madden, *ibid.* **58**, 6124 (1998).

²¹ N. Govind, Y. A. Wang, and E. A. Carter, J. Chem. Phys. **110**, 7677 (1999).

²² V. Shah, D. Nehete, and D. G. Kanhere, J. Phys.: Condens. Matter **6**, 10773 (1994); D. Nehete, V. Shah, and D. G. Kanhere, Phys. Rev. B **53**, 2126 (1996); V. Shah and D. G. Kanhere, J. Phys.: Condens. Matter **8**, L253 (1996); V. Shah, D. G. Kanhere, C. Majumber, and G. P. Das, *ibid.* **9**, 2165 (1997); A. Vichare and D. G. Kanhere, J. Phys.: Condens. Matter **10**, 3309 (1998); A. Vichare and D. G. Kanhere, Eur. Phys. J. D **4**, 89 (1998); A. Dhavale, V. Shah, and D. G. Kanhere, Phys. Rev. A **57**, 4522 (1998).

²³ N. Govind, J. L. Mozos, and H. Guo, Phys. Rev. B **51**, 7101 (1995); Y. A. Wang, N. Govind, and E. A. Carter, *ibid.* **58**, 13465 (1998).

²⁴ V. Bonacić-Koutecký, J. Jellinek, M. Wiechert, and P. Fantucci, J. Chem. Phys. **107**, 6321 (1997); D. Reichardt, V. Bonacić-Koutecký, P. Fantucci, and J. Jellinek, Chem. Phys. Lett. **279**, 129 (1997).

²⁵ S. Kümmel, P.-G. Reinhard, and M. Brack, Eur. Phys. J. D **9**, 149 (1999); S. Kümmel, M. Brack, and P.-G. Reinhard, unpublished results.

²⁶ I. L. Garzón, K. Michaelian, M. R. Beltrán, A. Posada-Amarillas, P. Ordejón, E. Artacho, D. Sánchez-Portal, and J. M. Soler, Phys. Rev. Lett. **81**, 1600 (1998).

²⁷ J. M. Soler, M. R. Beltrán, K. Michaelian, I. L. Garzón, P. Ordejón, D. Sánchez-Portal, and E. Artacho, Phys. Rev. B **61**, 5771 (2000).

²⁸ J. P. K. Doye and D. J. Wales, J. Phys. B **29**, 4859 (1996).

²⁹ *Theory of the inhomogeneous electron gas*. Editors S. Lundqvist and N. H. March. Plenum Press, New York (1983).

³⁰ W. Yang, Phys. Rev. A **34**, 4575 (1986).

³¹ J. P. Perdew, Phys. Lett. A **165**, 79 (1992).

³² J. P. Perdew and A. Zunger, Phys. Rev. B **23**, 5048 (1981).

³³ D. Ceperley and B. Alder, Phys. Rev. Lett. **45**, 566 (1980).

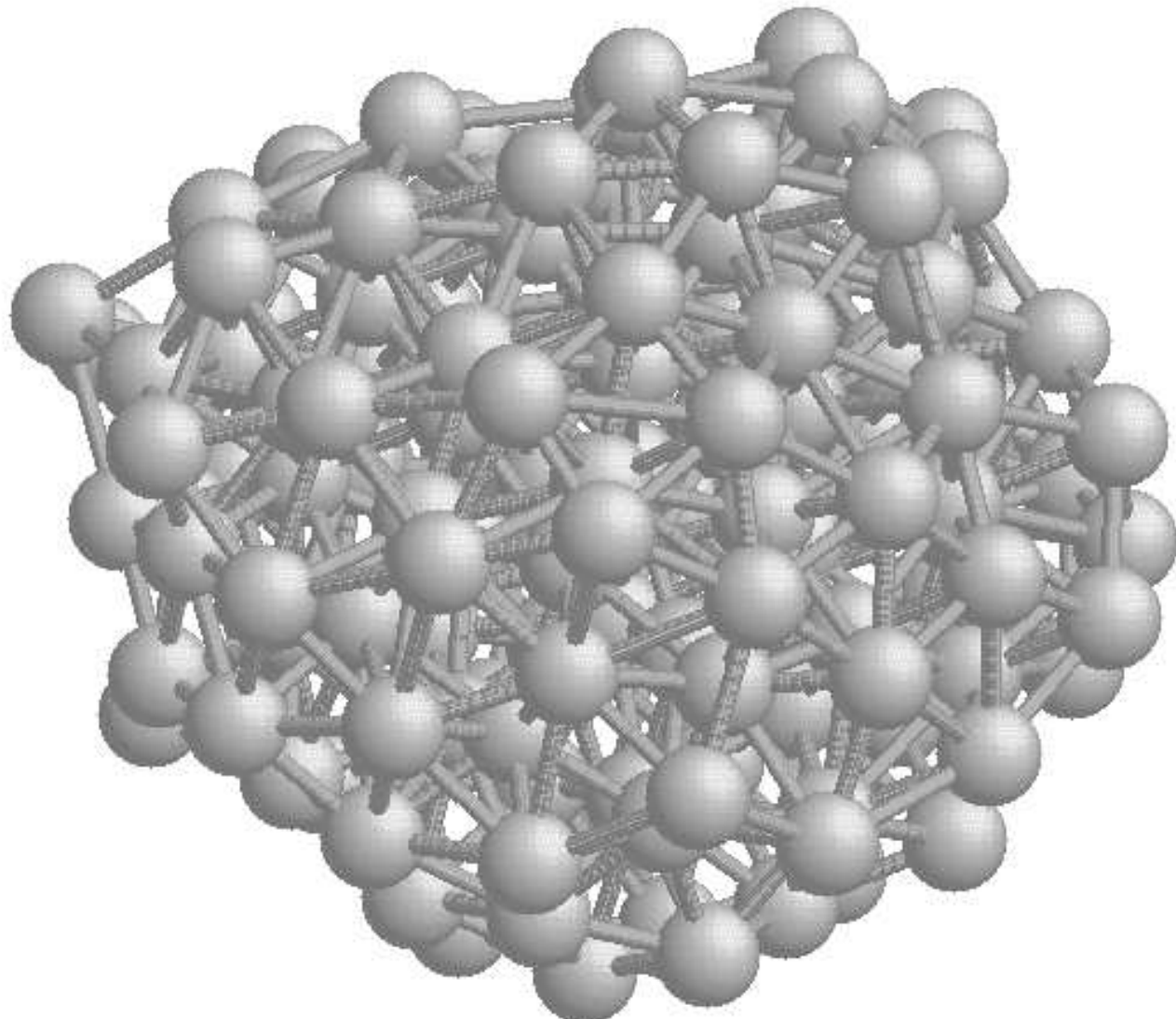
³⁴ C. Fiolhais, J. P. Perdew, S. Q. Armster, J. M. McLaren, and H. Brajczewska, Phys. Rev. B **51**, 14001 (1995); *ibid.* **53**, 13193 (1996).

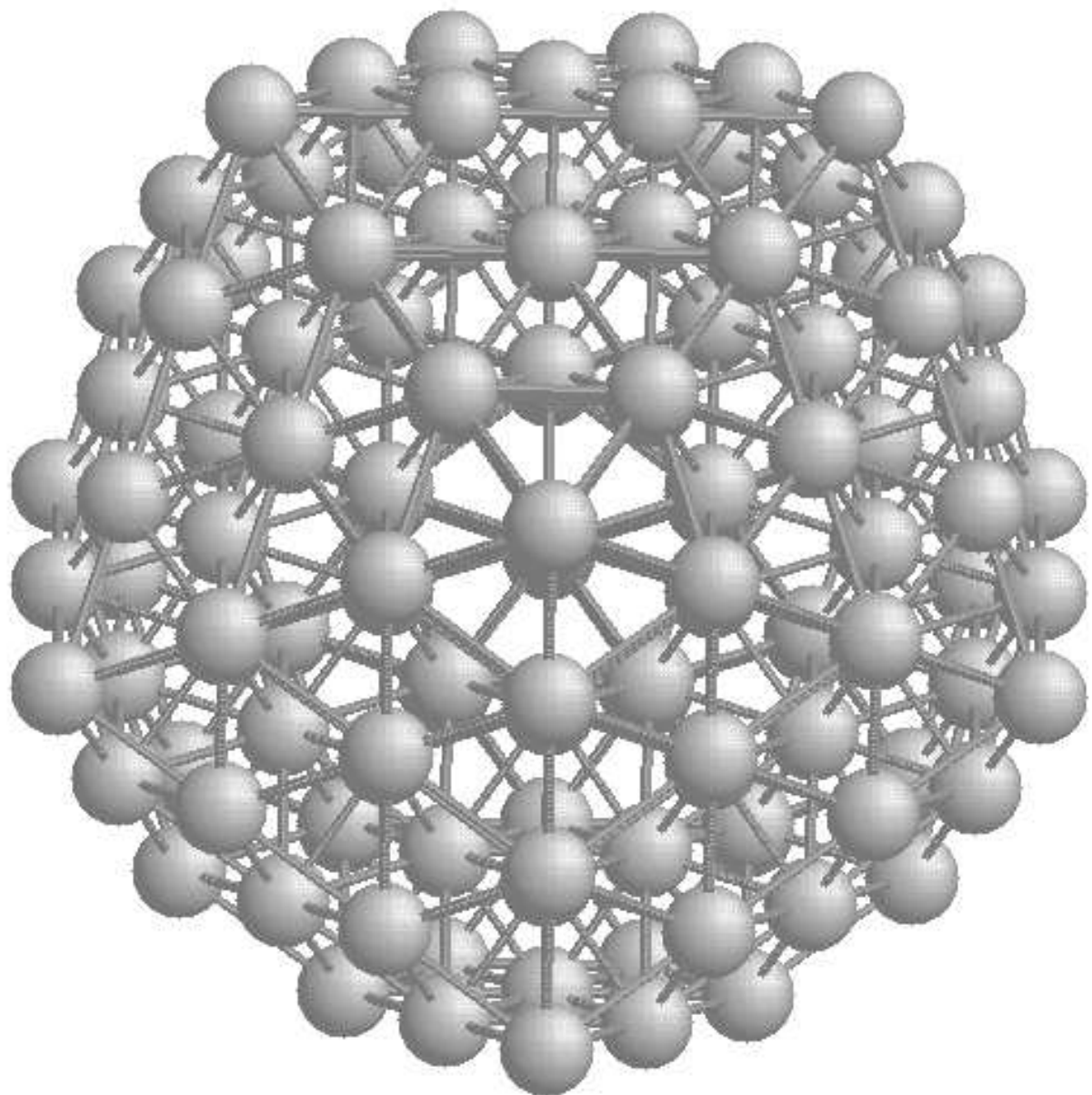
³⁵ F. Nogueira, C. Fiolhais, J. He, J. P. Perdew, and A. Rubio, J. Phys.: Condens. Matter **8**, 287 (1996).

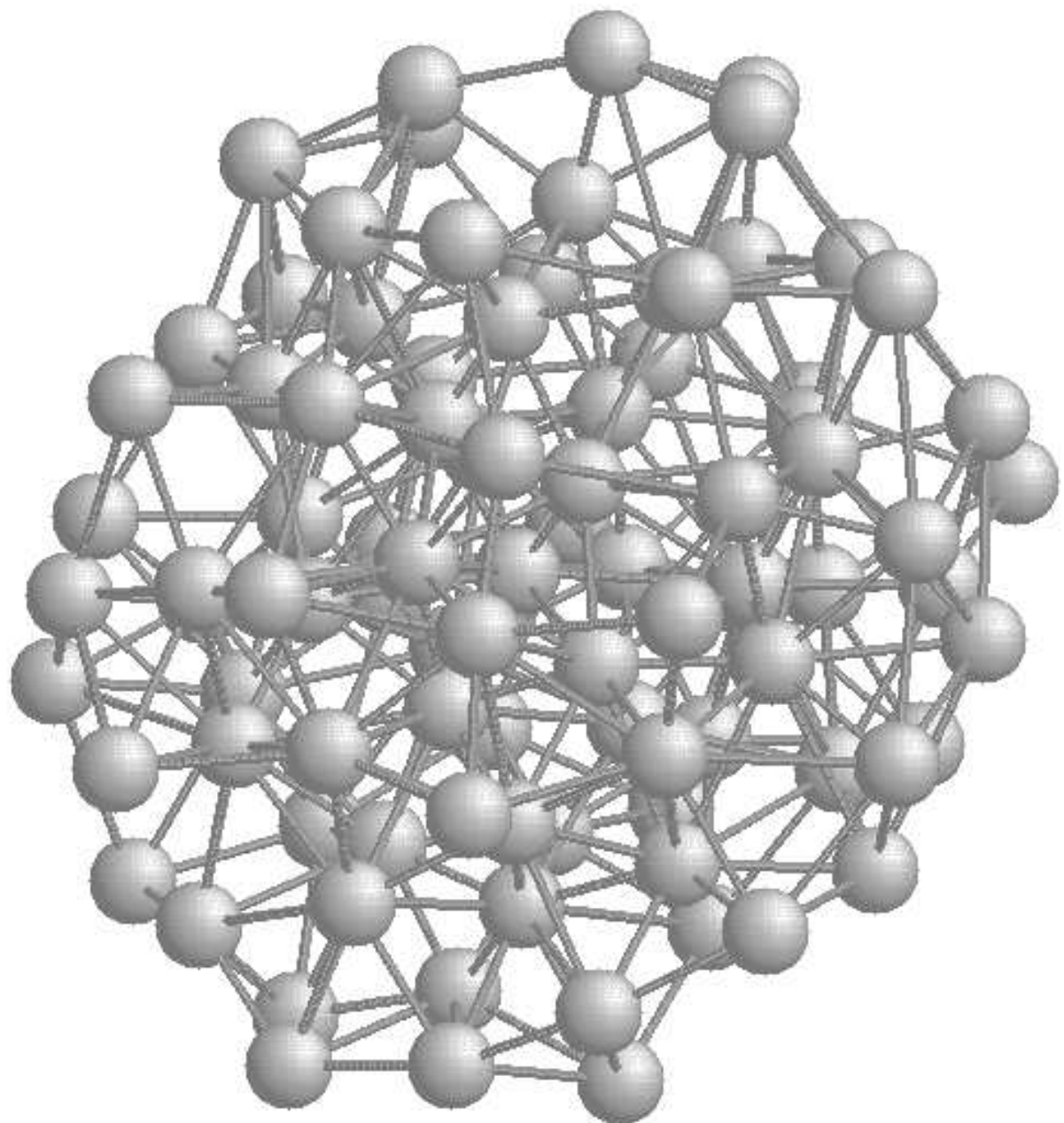
³⁶ L. Verlet, Phys. Rev. **159**, 98 (1967); W. C. Swope and H. C. Andersen, J. Chem. Phys. **76**, 637 (1982).

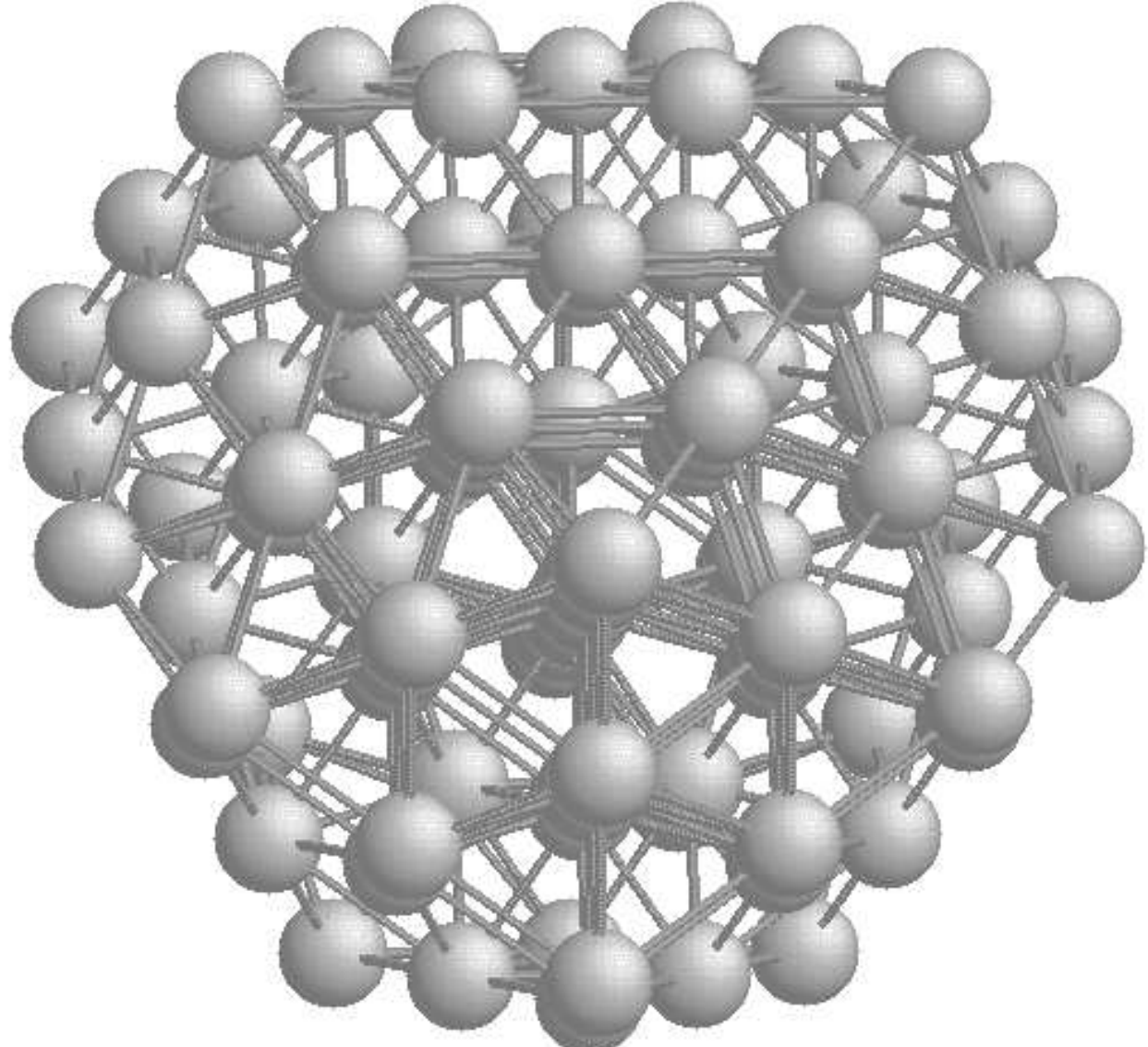
³⁷ S. Sugano, *Microcluster Physics*, Springer-Verlag, Berlin (1991).

³⁸ F. Ercolessi, W. Andreoni, and E. Tosatti, Phys. Rev. Lett. **66**, 911 (1991).

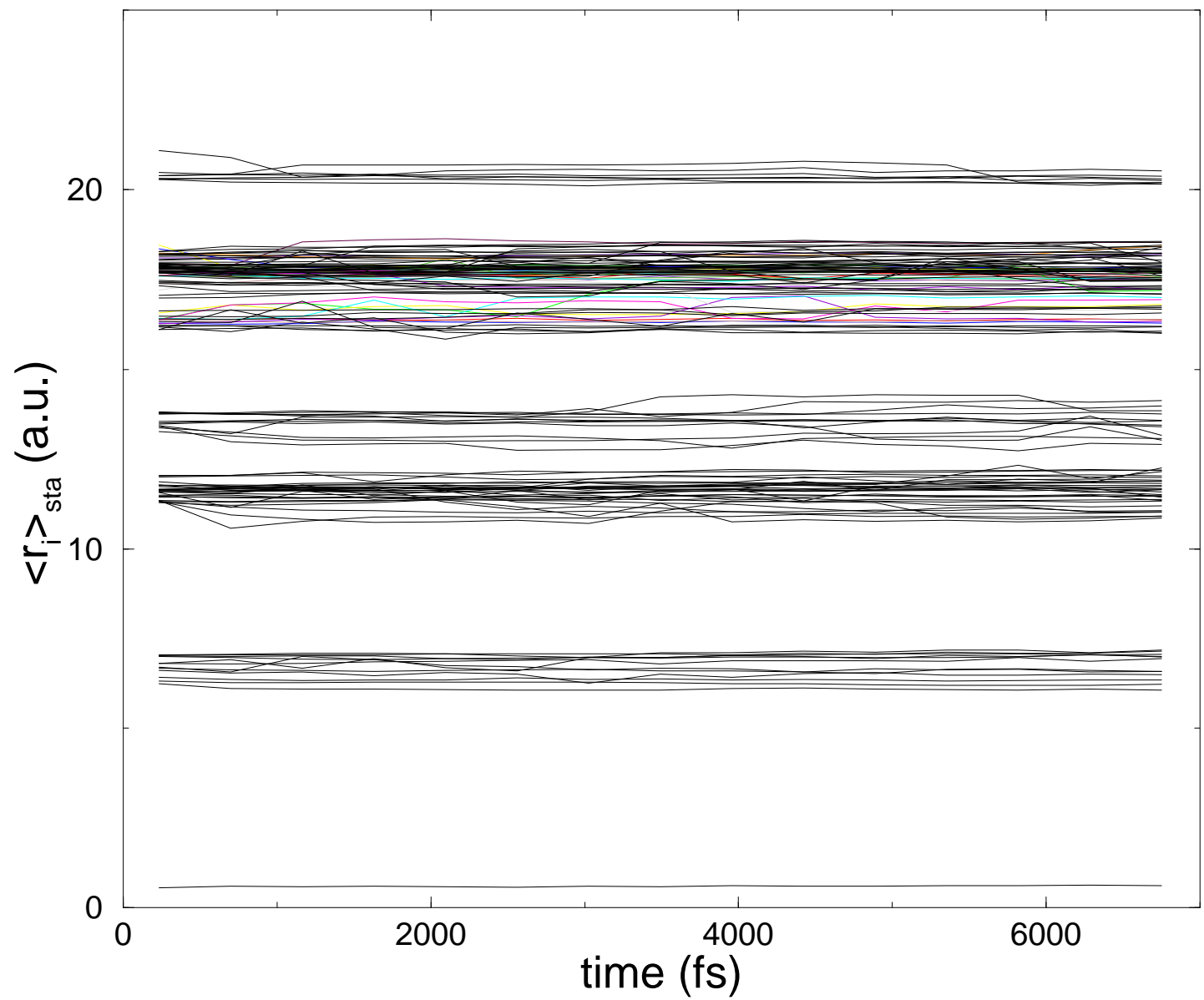


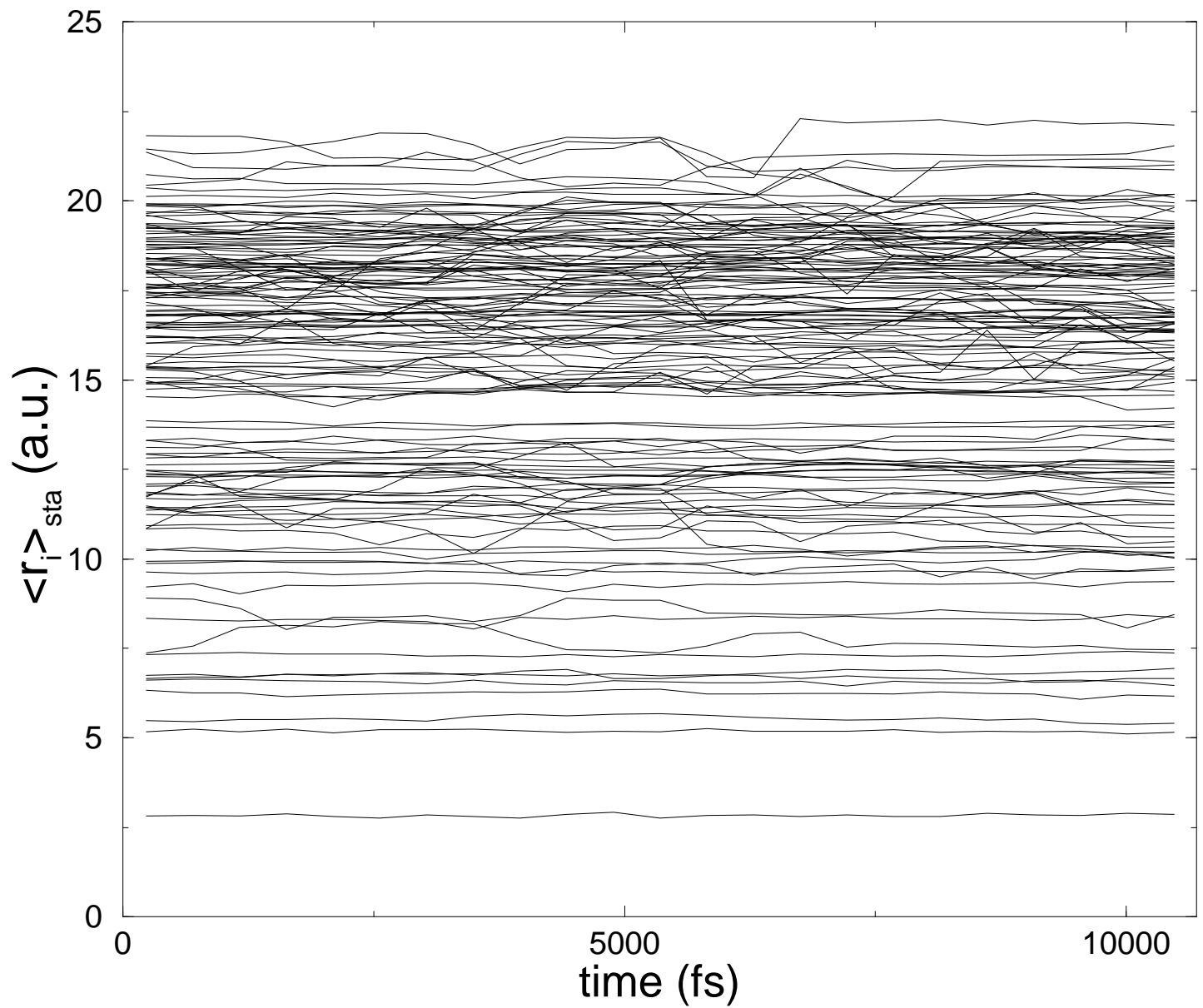






12





14

